Universität des Saarlandes

Fachrichtung 6.1 – Mathematik

Preprint Nr. 365

Morphological Counterparts of Linear Shift-Invariant Scale-Spaces

Martin Schmidt and Joachim Weickert

Saarbrücken 2016

Fachrichtung 6.1 – Mathematik
Universität des Saarlandes

Preprint No. 365
submitted: September 26, 2015
revised: February 10, 2016

Morphological Counterparts of Linear Shift-Invariant Scale-Spaces

Martin Schmidt

Mathematical Image Analysis Group,
Faculty of Mathematics and Computer Science,
Saarland University, Campus E1.7, 66041 Saarbrücken, Germany
schmidt@mia.uni-saarland.de

Joachim Weickert

Mathematical Image Analysis Group,
Faculty of Mathematics and Computer Science,
Saarland University, Campus E1.7, 66041 Saarbrücken, Germany
weickert@mia.uni-saarland.de

Edited by
FR 6.1 – Mathematik
Universität des Saarlandes
Postfach 15 11 50
66041 Saarbrücken
Germany

Fax: + 49 681 302 4443
e-Mail: preprint@math.uni-sb.de
WWW: http://www.math.uni-sb.de/

Abstract

It is well-known that there are striking analogies between linear shift-invariant systems and morphological systems for image analysis. So far, however, the relations between both system theories are mainly understood on a pure convolution / erosion level. A formal connection on the level of differential or pseudodifferential equations and their induced scale-spaces is still missing. The goal of our paper is to close this gap. We present a simple and fairly general dictionary that allows to translate any linear shift-invariant evolution equation into its morphological counterpart and vice versa. It is based on a scale-space representation by means of the symbol of its (pseudo)differential operator. Introducing a novel transformation, the Cramér–Fourier transform, puts us in a position to relate the symbol to the structuring function of a morphological scale-space of Hamilton–Jacobi type. As an application of our general theory, we derive the morphological counterparts of many linear shift-invariant scale-spaces, such as the Poisson scale-space, α-scale-spaces, summed α-scale-spaces, relativistic scale-spaces, and their anisotropic variants. Our findings are illustrated by experiments.

1 Introduction

Linear system theory and mathematical morphology are two successful and widely-used concepts in signal and image processing, and attempts to establish connections between these paradigms are undergoing since about three decades [43]. It is well-known that any linear shift-invariant system can be described as a convolution that can be computed elegantly as multiplication in the Fourier domain [40, 46]. On the other hand, morphological systems are based on erosions (or dilations) with a concave structuring function, which comes down to additions in the slope domain [42, 16]. An explanation for the quasi-logarithmic connection between both worlds has been obtained by Burgeth and Weickert [12]: While linear system theory uses the classical algebra $(\mathbb{R}, \cdot, +)$, they showed that mathematical morphology is a system theory in the min-plus algebra $(\mathbb{R} \cup \{+\infty\}, +, \min)$. Moreover, they described this relation by means of the Cramér transform. In the context of decision theory, this connection has been analysed by Akian et al. [2]. However, since their formulation would lead to divergent integrals we have to persue a different strategy.

Both linear and morphological systems are used for constructing so called scale-spaces. They embed an image into a family of gradually smoother representations [26, 63]. Studying the hierarchy over scale (deep structure) within such a scale-space allows to pass from a pure pixel-based description to a more semantic reasoning about the actual image content [45]. Moreover, scale-space ideas build the backbone of widely-used feature descriptors such as SIFT [39]. Alvarez et al. [3] have shown that under a reasonable set of axioms, scale-spaces are governed by evolution equations. Often they can be expressed as continuous-scale descriptions of linear or morphological systems in terms of partial differential equations (PDEs). For example, Gaussian convolution comes down to a homogeneous diffusion equation, whose evolution in time creates the so-called Gaussian scale-space [26, 63, 34]. More recently, linear scale-spaces based on pseudodifferential operators have attracted attention, such as the Poisson scale-space [20], α-scale-spaces [19], summed α-scale-spaces [14], and relativistic scale-spaces [11]. Also regularisation methods and related concepts can be interpreted as scale-spaces by considering their Euler-Lagrange equations, both in the linear and the nonlinear setting [50, 44, 53, 10, 13]. Since Gaussian scale-space can be described by a linear diffusion equation, it is natural to generalise it also to nonlinear diffusion scale-spaces [49, 60]. On the morphological side, continuous-scale versions of erosions are given by hyperbolic PDEs [3, 6, 9, 59]. Parabolic morphological PDEs comprise mean curvature motion [4, 33] which can be derived from iterated median filtering [23]. It is also possible to construct affine invariant morphological scale-spaces [3, 52]. Moreover, morphological variants of linear and nonlinear diffusion scale-spaces can be created by embedding these scale-spaces into a counter-harmonic framework [5].

An interesting equivalence between Gaussian scale-space and morphological erosion with a quadratic structuring function has been discovered by van den Boomgaard [58]: While Gaussians are the only separable and rotationally invariant convolution kernels [47], quadratic functions are the only separable and rotationally invariant structuring functions. This has also triggered Florack et al. [22] and Welk [62] to consider evolutions that combine both scale-spaces. However, other formal equivalences between the (pseudo)differential operators governing linear shift-invariant scale-spaces and morphological scale-spaces are not known so far.

Goal of the Paper. The goal of our paper is to address this problem. We establish a general theory that allows to transform a scale-space evolution from one of these worlds to the other world. On the one hand, this framework extends the results of Burgeth and Weickert [12] to differential and pseudodifferential operators. On the other hand, it allows to transfer the results of Akian et al. [2] to a scale-space and image processing setting. In particular, it enables us to derive the morphological counterparts of the Poisson scale-space, α-scale-spaces, summed α-scale-spaces, relativistic scale-spaces, and anisotropic variants of them. To this end, we characterise linear shift-invariant scale-spaces by their symbol. There is a one-to-one relation between the symbol and its corresponding convolution kernel. On the other hand, we express morphological scale-spaces by Hamilton-Jacobi equations whose viscosity solution is given by an infimal convolution with a suitable structuring function. Introducing a novel transformation that we call Cramér–Fourier transform allows us to connect convolutions and infimal convolutions and therefore also linear and morphological scale-spaces. We will see that this is most easily done on the level of their evolution equations, where we come up with a very simple and general dictionary.

The present paper relies on our SSVM 2015 conference paper [54]. Apart from more detailed explanations and more references, it extends the conference paper in several important aspects:

- Compared to [54], our theory is completely revised. Formulations based on the symbol, Hamilton-Jacobi equations, and infimal convolutions are not present in [54]. They allow a simpler, more transparent and more general theory.

- Simplicity is reflected by the fact that our dictionary allows to translate results between the linear and the morphological world directly on the level of evolution equations via the symbol. In [54], we had to achieve this goal in an indirect and more cumbersome way by computing the infinitesimal generator of a structuring function.

- Transparency is improved e.g. by introducing clear formal definitions of morphological counterparts of linear shift-invariant evolutions, both on a convolution / infimal convolution level and an evolution equation level.

- To illustrate greater generality, we cover additional scale-spaces that have not been discussed in [54], such as summed α-scale-spaces and anisotropic variants of Gaussian and Poisson scale-space.

Paper Structure. Sections 2 and 3 reinterpret relevant concepts behind linear shift-invariant scale-spaces and morphological scale-spaces in a way that allows us to derive our general framework in Section 4. The fifth Section applies our theory to various scale-spaces. Experiments in Section 6 illustrate their behaviour. Our paper is concluded with a summary in Section 7.

2 Linear Shift-Invariant Scale-Spaces

The goal of this section is to provide a general framework for linear shift-invariant scale-spaces in terms of an evolution that is steered by a pseudodifferential operator. This operator also induces a corresponding convolution kernel. We will see that the so-called symbol carries the essential information of both scale-space representation.

2.1 Scale-Spaces as Pseudodifferential Evolutions

Throughout this paper, let us consider some bounded greyscale image $f\colon \mathbb{R}^2 \to \mathbb{R}$. A scale-space representation of f embeds this image into a family $u(.,t)$ of gradually smoother versions, where the scale parameter ("time") t determines the amount of smoothing or image simplification: $t = 0$ yields $u(.,0) = f$, and larger values for t correspond to simpler versions of f with less structure. Reasonable scale-spaces have to satisfy a number of architectural properties, simplification qualities, and invariances [3]. Typically their evolutions w.r.t. the scale-parameter t can be expressed in terms of differential or pseudodifferential equations.

To define pseudodifferential operators mathematically we follow [56]. However, we use a different convention for the Fourier transform of an image u:

$$\hat{u}(\boldsymbol{\xi}) := \mathcal{F}[u](\boldsymbol{\xi}) := \int_{\mathbb{R}^2} u(\boldsymbol{x})\, e^{-2\pi \mathrm{i} \langle \boldsymbol{\xi}, \boldsymbol{x} \rangle}\, d\boldsymbol{x} \tag{1}$$

where $\mathrm{i}^2 = -1$ and $\langle .,. \rangle$ denotes the Hermitian inner product. The Fourier backtransform is given by

$$u(\boldsymbol{x}) = \mathcal{F}^{-1}\left[\, \hat{u} \,\right](\boldsymbol{x}) := \int_{\mathbb{R}^2} \hat{u}(\boldsymbol{\xi})\, e^{2\pi \mathrm{i} \langle \boldsymbol{x}, \boldsymbol{\xi} \rangle}\, d\boldsymbol{\xi}\ . \tag{2}$$

For a multi-index $\boldsymbol{\alpha} = (\alpha_1, \alpha_2) \in \mathbb{N}^2$ and some vector $\boldsymbol{v} \in \mathbb{R}^2$ we define $|\boldsymbol{\alpha}| := \alpha_1 + \alpha_2$ and $\boldsymbol{v}^{\boldsymbol{\alpha}} := v_1^{\alpha_1}\, v_2^{\alpha_2}$. Then differentiation yields

$$\boldsymbol{\nabla}^{\boldsymbol{\alpha}} u(\boldsymbol{x}) = \int_{\mathbb{R}^2} (2\pi \mathrm{i}\, \boldsymbol{\xi})^{\boldsymbol{\alpha}}\ \hat{u}(\boldsymbol{\xi})\, e^{2\pi \mathrm{i} \langle \boldsymbol{x}, \boldsymbol{\xi} \rangle}\, d\boldsymbol{\xi} \tag{3}$$

where $\boldsymbol{\nabla}$ denotes the spatial gradient $(\partial_x, \partial_y)^\top$. For a differential operator

$$P(\boldsymbol{x}, \boldsymbol{\nabla}) = \sum_{|\boldsymbol{\alpha}| \le k} c_{\boldsymbol{\alpha}}(\boldsymbol{x}) \boldsymbol{\nabla}^{\boldsymbol{\alpha}} \tag{4}$$

this implies

$$P(\boldsymbol{x}, \boldsymbol{\nabla})u(\boldsymbol{x}) = \int_{\mathbb{R}^2} p\left(\boldsymbol{x}, 2\pi\,\boldsymbol{\xi}\right)\, \hat{u}(\boldsymbol{\xi})\, e^{2\pi \mathrm{i} \langle \boldsymbol{x}, \boldsymbol{\xi} \rangle}\, d\boldsymbol{\xi}\,, \tag{5}$$

where the polynomial

$$p(\boldsymbol{x}, \boldsymbol{\xi}) = \sum_{|\boldsymbol{\alpha}| \leq k} c_{\boldsymbol{\alpha}}(\boldsymbol{x})(\mathrm{i}\,\boldsymbol{\xi})^{\boldsymbol{\alpha}} \tag{6}$$

is called the *symbol* of $P(\boldsymbol{x}, \boldsymbol{\nabla})$. If p is not a polynomial, Equation (5) can be used to define so called pseudodifferential operators. Since we are interested in shift-invariant systems, we focus on pseudodifferential equations with constant coefficients. In this case, p does not depend on $\boldsymbol{x}$. Therefore, we drop the first argument and write $p(\boldsymbol{\xi})$ and $P(\boldsymbol{\nabla})$. Then the scale-space evolutions are given by

$$\boxed{\begin{aligned} \partial_t u(\boldsymbol{x}, t) &= P(\boldsymbol{\nabla})u(\boldsymbol{x}, t) && (7) \\ u(\boldsymbol{x}, 0) &= f(\boldsymbol{x})\ . && (8) \end{aligned}}$$

We call linear shift-invariant (LSI) evolutions of this type *LSI scale-spaces.* As we shall see below, they comprise many well-known linear scale-spaces.

2.2 Interpretation as Convolution Scale-Spaces

Let us now interpret LSI scale-spaces in terms of convolutions with appropriate kernels. Since Equation (7) is linear, it can be described by a multiplication in the Fourier domain where the factor is given by the symbol. To see this, we apply the Fourier transform to (5) and obtain

$$\mathcal{F}\left[\, P(\boldsymbol{\nabla})u(\cdot, t)\,\right](\boldsymbol{\xi}) = p(2\pi\,\boldsymbol{\xi})\hat{u}(\boldsymbol{\xi}, t)\,. \tag{9}$$

Therefore, (7)–(8) simplifies under the Fourier transform to the initial value problem

$$\partial_t \hat{u}(\boldsymbol{\xi}, t) = p(2\pi\,\boldsymbol{\xi})\hat{u}(\boldsymbol{\xi}, t)\,, \tag{10}$$

$$\hat{u}(\boldsymbol{\xi}, 0) = \hat{f}(\boldsymbol{\xi})\,. \tag{11}$$

Its solution is given by

$$\hat{u}(\boldsymbol{\xi}, t) = \hat{f}(\boldsymbol{\xi})\ \exp\left(p(2\pi\,\boldsymbol{\xi})\, t\right)\ . \tag{12}$$

Applying the inverse Fourier transform translates the result to the spatial domain again:

$$u(\boldsymbol{x}, t) = \big(f * \mathcal{F}^{-1} [\exp(p(2\pi\,\cdot)\,t)]\big)(\boldsymbol{x})\,. \tag{13}$$

This shows the importance of the symbol p: We can use it to characterise the solution of (7)–(8) as a convolution of the initial image $f(\boldsymbol{x})$ with an appropriate kernel $k(\boldsymbol{x}, t)$:

$$\boxed{\begin{aligned} u(\boldsymbol{x}, t) &= (f * k(\cdot, t))\,(\boldsymbol{x}), & (14)\\ k(\boldsymbol{x}, t) &= \mathcal{F}^{-1} [\exp(p(2\pi\,\cdot)\,t)]\,(\boldsymbol{x}). & (15) \end{aligned}}$$

2.3 Examples of LSI Scale-Spaces

In order to illustrate that the family of LSI scale-spaces is fairly rich, let us investigate five examples in more detail.

1. **Gaussian Scale-Space.** It computes smoothed versions $u(\boldsymbol{x}, t)$ of $f(\boldsymbol{x})$ as solutions of the initial value problem

$$\partial_t u = \Delta u \qquad \text{on } \mathbb{R}^2 \times (0, \infty), \tag{16}$$

$$u(\boldsymbol{x}, 0) = f(\boldsymbol{x}) \qquad \text{on } \mathbb{R}^2, \tag{17}$$

   where $\Delta = \partial_{xx} + \partial_{yy}$ denotes the spatial Laplacian. Gaussian scale-space goes back to Iijima [26, 61]. It became popular in the western world by the work of Witkin [63], Koenderink [34], Lindeberg [36], Florack [21], and many others; see e.g. [55] and the references therein.

2. α**-Scale-Spaces.** These evolutions replace the homogeneous diffusion equation (16) by the pseudodifferential equation

$$\partial_t u = -(-\Delta)^\alpha u \tag{18}$$

   with some parameter $\alpha \in (0, \infty)$. While such processes can already be found implicitly in Iijima's early work [26] and more explicitly e.g. in a publication by Pauwels et al. [48], they became popular as scale-spaces due to the work of Duits et al. [19]. Gaussian scale-space is recovered for $\alpha = 1$, while $\alpha = \frac{1}{2}$ gives the so-called Poisson scale-space

$$\partial_t u = -\sqrt{-\Delta}\, u \tag{19}$$

   of Felsberg and Sommer [20]. If one renounces a maximum–minimum principle, one can also study scale-spaces for $\alpha > 1$, comprising e.g. the biharmonic scale-space for $\alpha = 2$ [14].

3. **Summed α-Scale-Spaces.** Didas et al. [14] discuss finite linear combinations of fractional Laplacians:

$$\partial_t u = -\sum_{k=1}^{m} \lambda_k (-\Delta)^{\alpha_k} u \tag{20}$$

with fractional derivative orders $\alpha_1, \ldots, \alpha_m > 0$ and weights $\lambda_1, \ldots, \lambda_m > 0$. Interestingly they can satisfy a maximum–minimum principle even if some terms with $\alpha > 1$ are present, as long as they are dominated by terms with $\alpha < 1$.

The special case of a linear combination of one Gaussian and one Poisson kernel is used in [32] to approximate α-scale-spaces.

4. **Relativistic Scale-Spaces.** Burgeth et al. [11] have advocated a generalisation of the Poisson scale-space by considering the evolution equations

$$\partial_t u = -\left(\sqrt{m^2 - \Delta} - m\right) u \tag{21}$$

with $m \geq 0$. We see that this family contains the Poisson scale-space for $m = 0$.

5. **Anisotropic Scale-Spaces.** Formally one can construct anisotropic versions of any of the preceding scale-spaces by replacing their Laplacian by $\boldsymbol{\nabla}^\top \boldsymbol{D}\, \boldsymbol{\nabla}$ with some symmetric positive definite matrix $\boldsymbol{D} \in \mathbb{R}^{2\times 2}$. In the case of Gaussian scale-space, this leads to the anisotropic Gaussian scale-spaces

$$\partial_t u = \operatorname{div}\left(\boldsymbol{D}\, \boldsymbol{\nabla} u\right). \tag{22}$$

They have been derived axiomatically by Iijima [27, 28] and later on by Lindeberg [36, 37]. Scale-space properties of nonlinear variants where the diffusion tensor $\boldsymbol{D}$ is a function of the local structure of the evolving image are investigated in [60].

Although these scale-spaces differ w.r.t. decay behaviour in Fourier space, separability, extremum principle, nonenhancement of local extrema and scale invariance, the pseudodifferential operators $P(\boldsymbol{\nabla})$ and their corresponding kernels $k(\boldsymbol{x}, t)$ can be computed following the strategy in Subsections 2.1 and 2.2. The results are summarised in Table 1. Note that the symbol representation allows simple formulas even in those cases where the corresponding kernels do not have a closed form representation. Therefore, we will also use it later on for establishing correspondences to morphological scale-spaces.

Table 1: Specific LSI scale-spaces, their evolution equations, symbols, and convolution kernels. Γ denotes the gamma function, and K_ν is the modified Bessel function of the third kind [1].

LSI scale-space	evolution equation	symbol	kernel
alpha	$\partial_t u = -(-\Delta)^\alpha u$	$p(\boldsymbol{\xi}) = -\lvert\boldsymbol{\xi}\rvert^{2\alpha}$	no closed formula
Gaussian	$\partial_t u = \Delta u$	$p(\boldsymbol{\xi}) = -\lvert\boldsymbol{\xi}\rvert^{2}$	$k(\boldsymbol{x},t) = \frac{1}{4\pi t}\exp\left(-\frac{\lvert\boldsymbol{x}\rvert^2}{4t}\right)$
Poisson	$\partial_t u = -\sqrt{-\Delta}\, u$	$p(\boldsymbol{\xi}) = -\lvert\boldsymbol{\xi}\rvert$	$k(\boldsymbol{x},t) = \frac{\Gamma(\frac{3}{2})}{\pi^{3/2}}\,\frac{t}{(t^2+\lvert\boldsymbol{x}\rvert^2)^{3/2}}$
summed alpha	$\partial_t u = -\sum_{k=1}^{m} \lambda_k(-\Delta)^{\alpha_k} u$	$p(\boldsymbol{\xi}) = -\sum_{k=1}^{m} \lambda_k \lvert\boldsymbol{\xi}\rvert^{2\alpha_k}$	no closed formula
relativistic	$\partial_t u = \left(m - \sqrt{m^2-\Delta}\,\right) u$	$p(\boldsymbol{\xi}) = m - \sqrt{m^2+\lvert\boldsymbol{\xi}\rvert^2}$	$k(\boldsymbol{x},t) = \left(\frac{m}{2\pi}\right)^{\frac{3}{2}} \frac{2t\,e^{tm}}{(t^2+\lvert\boldsymbol{x}\rvert^2)^{3/4}}\, K_{\frac{3}{2}}\left(m\sqrt{t^2+\lvert\boldsymbol{x}\rvert^2}\right)$
anis. Gaussian	$\partial_t u = \operatorname{div}(\boldsymbol{D}\,\boldsymbol{\nabla} u)$	$p(\boldsymbol{\xi}) = -\langle \boldsymbol{\xi}, \boldsymbol{D}\,\boldsymbol{\xi}\rangle$	$k(\boldsymbol{x},t) = \frac{1}{4\pi t \det \boldsymbol{D}}\exp\left(-\frac{\boldsymbol{x}^\top \boldsymbol{D}^{-1}\boldsymbol{x}}{4t}\right)$

3 Morphological Scale-Spaces

In this section we want to introduce another class of scale-spaces, called morphological scale-spaces. To emphasise the similarities and differences to the linear scale-spaces from Section 2, we keep the general structure as similar as possible.

3.1 Morphological Scale-Spaces as Evolution Equations

Mathematical morphology is a system theory where the classical algebra $(\mathbb{R}, \times, +)$ that is used within linear system theory is replaced by the morphological min-plus algebra $\mathbb{R}_{\min} := (\mathbb{R} \cup \{+\infty\}, +, \min)$. For more details we refer to [12]. In the last decades, min-plus and max-plus algebras have become very fruitful tools in applications such as discrete event systems [7], and they have been studied also from a more theoretical perspective in fields like tropical geometry [41].

Following Heijmans and Maragos [25], we consider *Hamilton-Jacobi equations* of type

$$\boxed{\begin{aligned} \partial_t v &= -H(\boldsymbol{\nabla} v), \qquad (23)\\ v(\boldsymbol{x},0) &= f(\boldsymbol{x}) \qquad (24)\end{aligned}}$$

as evolutions that lead to morphological scale-spaces. In the sequel, we will assume that f is bounded and *lower semi-continuous (lsc)*, i.e.

$$f(\boldsymbol{x}_0) \leq \lim_{\boldsymbol{x}\to\boldsymbol{x}_0} \inf f(\boldsymbol{x}) \qquad\qquad \text{for all } \boldsymbol{x}_0, \tag{25}$$

and the function H is convex and *coercive*, i.e.

$$\lim_{|\boldsymbol{x}|\to\infty} \frac{H(\boldsymbol{x})}{|\boldsymbol{x}|} = \infty\,. \tag{26}$$

Under these conditions, the initial value problem (23)–(24) has a unique viscosity solution [38].
For our morphological systems, the problem (23)–(24) plays the same role as problem (7)–(8) does for LSI systems.

3.2 Interpretation as Infimal Convolution Scale-Spaces

As described e.g. in [24], the unique viscosity solution of (23)–(24) is given by the *Hopf-Lax formula*

$$v(\boldsymbol{x},t) = \min_{\boldsymbol{y}\in\mathbb{R}^2} \left\{ f(\boldsymbol{y}) + t\,H^*\left(\frac{\boldsymbol{x}-\boldsymbol{y}}{t}\right)\right\} \tag{27}$$

where H^* denotes the the convex conjugate of H:

$$s(\boldsymbol{x}) = H^*(\boldsymbol{x}) := \sup_{\boldsymbol{y}\in\mathbb{R}^2} \{\langle \boldsymbol{y},\boldsymbol{x}\rangle - H(\boldsymbol{y})\}. \tag{28}$$

We define the *structuring function (SF)*

$$s(\boldsymbol{x},t) := t\,H^*\left(\frac{\boldsymbol{x}}{t}\right) = (tH)^*(\boldsymbol{x}) \tag{29}$$

and use the notation of an *infimal convolution*

$$(f \,\square\, g)(\boldsymbol{x}) = \inf_{\boldsymbol{y}\in\mathbb{R}^2} \{f(\boldsymbol{y}) + g(\boldsymbol{x}-\boldsymbol{y})\}\ . \tag{30}$$

Then the solution of our morphological evolution is given by

$$\boxed{\begin{aligned} v(\boldsymbol{x},t) &= (f \,\square\, s(\cdot,t))(\boldsymbol{x})\,, \qquad (31)\\ s(\boldsymbol{x},t) &= (tH)^*(\boldsymbol{x})\,. \qquad (32)\end{aligned}}$$

3.3 Examples of Morphological Scale-Spaces

In a similar way as our LSI framework covers a large family of linear scale spaces, the Hamilton-Jacobi formulation comprises also many morphological scale-spaces. We illustrate this by a number of examples.

1. **Dilation and Erosion Scale-Spaces**

   Usually mathematical morphology is expressed in terms of dilations and erosions. The *dilation* $\oplus$ resp. *erosion* $\ominus$ of an image f with some structuring function $b : \mathbb{R}^2 \to \mathbb{R} \cup \{-\infty\}$ is defined as

   $$(f \oplus b)(\boldsymbol{x}) := \sup_{\boldsymbol{y} \in \mathbb{R}^2} \{f(\boldsymbol{y}) + b(\boldsymbol{x}-\boldsymbol{y})\}\,, \tag{33}$$

   $$(f \ominus b)(\boldsymbol{x}) := \inf_{\boldsymbol{y} \in \mathbb{R}^2} \left\{f(\boldsymbol{y}) + \bar{b}(\boldsymbol{x}-\boldsymbol{y})\right\} \tag{34}$$

   where the bar notation denotes $\bar{b}(\boldsymbol{x}) := -b(-\boldsymbol{x})$.
   Dilations and erosions are related to the infimal convolution by

   $$f \ominus b \;=\; f \;\Box\; \bar{b}\,, \tag{35}$$

   $$-(f \oplus b) = (-f)\,\Box\,(-b)\,. \tag{36}$$

   Therefore, infimal convolutions behave essentially like erosions. Dilations can be obtained by applying an infimal convolution with the negative of the structuring function to the negative of the signal.

   For these reasons, results for dilations and erosions are equivalent to results for infimal convolutions.

2. **Quadratic Structuring Function Scale-Space.** Taking $s(\boldsymbol{x}) = \frac{1}{4}|\boldsymbol{x}|^2$ as structuring function, equation (28) implies that $H(\boldsymbol{x}) = |\boldsymbol{x}|^2$. In this case, the infimal convolution

   $$v(\boldsymbol{x}, t) = (f \;\Box\; s(\cdot, t))\,(\boldsymbol{x}) \tag{37}$$

   is the viscosity solution of the evolution process

   $$\partial_t v = -|\boldsymbol{\nabla} v|^2\,, \tag{38}$$

   $$v(0) = f\,. \tag{39}$$

   Van den Boomgaard has shown that quadratic structuring functions such as

   $$s(\boldsymbol{x}) = \tfrac{1}{4}|\boldsymbol{x}|^2 \tag{40}$$

are the only structuring functions that are rotationally invariant and separable [58]. This has motivated him to regard (38)–(39) as the morphological equivalent of Gaussian scale-space, since the latter one is the only scale-space with a rotationally invariant and separable convolution kernel [47, 61].

3. **Scale-Spaces with Flat Disc Structuring Functions.** If one uses as structuring function a flat disc

$$s(\boldsymbol{x}) \;=\; \begin{cases} 0 & \text{for } |\boldsymbol{x}| \leq 1, \\ \infty & \text{else,} \end{cases} \tag{41}$$

it has been shown in [3, 6, 9] that one arrives at

$$\partial_t v = -|\boldsymbol{\nabla} v|. \tag{42}$$

Evolutions of this type can be interpreted in many ways as scale-spaces; see [3, 59, 31] for more details.

4. **Structuring Functions of Arbitrary Power.** Jackway [29] as well as Diop and Angulo [15] have investigated morphological processes that can be described by evolution equations of type

$$\partial_t v = -|\boldsymbol{\nabla} v|^{\beta} \tag{43}$$

with arbitrary powers $\beta > 1$. Their corresponding structuring functions are given by the poweroids

$$s(\boldsymbol{x}) = (\beta - 1)\, |\boldsymbol{x}/\beta|^{\beta/(\beta-1)}\ . \tag{44}$$

5. **Anisotropic Structuring Functions.** So far, all our morphological scale-spaces use isotropic structuring functions that do not favour specific directions. Depending on the application, it can make sense to consider also anisotropic structuring functions that are adapted to directions of special interest.
An early anisotropic morphological PDE model goes back to Arehart et al. [6]: They have used ellipse-shaped flat structuring functions

$$s(\boldsymbol{x}) = \begin{cases} 0 & \boldsymbol{x}^\top \boldsymbol{D}^{-1} \boldsymbol{x} \leq 1, \\ \infty & \text{else} \end{cases} \tag{45}$$

with some positive definite symmetric matrix $\boldsymbol{D}$. This leads to evolutions of type

$$\partial_t v = -|\boldsymbol{D}\,\boldsymbol{\nabla} v|\,. \tag{46}$$

Later on, Breuß et al. [8] have adapted $\boldsymbol{D}$ to the underlying local image structure.

Evolutions with anisotropic quadratic structuring functions

$$s(\boldsymbol{x}) = \frac{1}{4}\boldsymbol{x}^\top \boldsymbol{D}^{-1}\boldsymbol{x} \tag{47}$$

can be described by

$$\partial_t v = -\boldsymbol{\nabla}^\top v\,\boldsymbol{D}\,\boldsymbol{\nabla} v. \tag{48}$$

Such processes go back to van den Boomgaard [57] and Jackway [30] in a space-invariant setting. More recently, Landström [35] has considered space-adaptive generalisations.

Table 2 gives a compact representation of the morphological examples that we have discussed.

Table 2: Specific morphological scale-spaces of Hamilton-Jacobi type and their structuring functions (SFs).

morphological scale-space	evolution equation	structuring function
quadratic SF	$\partial_t v = -\|\boldsymbol{\nabla} v\|^2$	$s(\boldsymbol{x},t) = \frac{1}{4t}\|\boldsymbol{x}\|^2$
flat disk SF	$\partial_t v = -\|\boldsymbol{\nabla} v\|$	$s(\boldsymbol{x},t) = \begin{cases} 0 & \|\boldsymbol{x}\| \le t, \\ \infty & \text{else} \end{cases}$
poweroid SF	$\partial_t v = -\|\boldsymbol{\nabla} v\|^\beta$	$s(\boldsymbol{x},t) = t\,(\beta-1)\left\|\frac{\boldsymbol{x}}{t\beta}\right\|^{\beta/(\beta-1)}$
flat ellipse-shaped SF	$\partial_t v = -\|\boldsymbol{D}\,\boldsymbol{\nabla} v\|$	$s(\boldsymbol{x},t) = \begin{cases} 0 & \boldsymbol{x}^\top\boldsymbol{D}^{-1}\boldsymbol{x} \le t^2, \\ \infty & \text{else} \end{cases}$
anisotropic quadratic SF	$\partial_t v = -\boldsymbol{\nabla}^\top v\,\boldsymbol{D}\,\boldsymbol{\nabla} v$	$s(\boldsymbol{x},t) = \frac{1}{4t}\boldsymbol{x}^\top\boldsymbol{D}^{-1}\boldsymbol{x}$

4 Morphological Counterparts of Linear Scale-Spaces

In Section 2 we have seen that linear pseudodifferential equations with constant coefficients can be solved by means of convolutions. On the other hand, in Section 3 we have emphasised infimal convolutions as a tool for solving morphological PDEs. The goal of this section is to connect both worlds, first on a convolution / infimal convolution level and afterwards on the level of evolution equations. To this end, it is useful to introduce a novel transformation, the Cramér–Fourier transform.

4.1 Connections between Convolutions and Infimal Convolutions

Burgeth and Weickert [12] have explained connections between linear and morphological systems by considering the *Cramér transform*

$$\mathcal{C}\,[\,f\,] := \big(\log \mathcal{L}\,[\,f\,]\,\big)^*, \tag{49}$$

which relies on the (double sided) *Laplace transform*

$$\mathcal{L}\,[\,f\,]\,(\boldsymbol{x}) = \int_{\mathbb{R}^2} f(\boldsymbol{y}) e^{\langle \boldsymbol{x}, \boldsymbol{y} \rangle}\, d\boldsymbol{y}. \tag{50}$$

Unfortunately, the Laplace transform is only finite for functions with exponential decay, which limits its applicability in image processing.

As a remedy, we propose a variant of the Cramér transform that is based on the Fourier transform. This allows a wider applicability. We call our novel transformation the Cramér-Fourier transform and define it as follows:

Definition 1. *Let f be a function with a real-valued and nonnegative Fourier transform. Then its* Cramér-Fourier transform *is given by*

$$\mathcal{C}_{\mathcal{F}}\,[\,f\,] := \big(-\log \mathcal{F}\,[\,f\,]\,\big(\tfrac{\cdot}{2\pi}\big)\,\big)^*. \tag{51}$$

This definition fits well to our kernels in Table 1: Their Fourier transform is real-valued (due to the kernel symmetry) and positive.

First we prove that the Cramér-Fourier transform benefits from the same key property as the classical Cramér transform considered in [12]: It maps convolutions to infimal convolutions.

Theorem 1 (Convolution Property of the Cramér-Fourier transform)**.** *Assume that two functions f and g are proper, lower semi-continuous, and have convex Cramér-Fourier transforms. Then the following holds true:*

$$\mathcal{C}_{\mathcal{F}}\,[\,f * g\,] \;=\; \mathcal{C}_{\mathcal{F}}\,[\,f\,] \,\Box\, \mathcal{C}_{\mathcal{F}}\,[\,g\,]. \tag{52}$$

Proof. Our proof uses several results from convex analysis (see e.g. [51]). Since $\mathcal{C}_{\mathcal{F}}[\,f\,]$ and $\mathcal{C}_{\mathcal{F}}[\,g\,]$ are lsc, proper and convex, also their convex conjugates $\mathcal{C}_{\mathcal{F}}[\,f\,]^*$ and $\mathcal{C}_{\mathcal{F}}[\,g\,]^*$ share these properties. Moreover, it follows that $\mathcal{C}_{\mathcal{F}}[\,f\,]^* = -\log \mathcal{F}[\,f\,]$. Therefore, a direct computation gives

$$\begin{aligned}
\mathcal{C}_{\mathcal{F}}[\,f * g\,] &= \left(-\log \mathcal{F}[\,f * g\,]\left(\tfrac{\cdot}{2\pi}\right)\right)^* \\
&= \left((-\log \mathcal{F}[\,f\,]\left(\tfrac{\cdot}{2\pi}\right)) + (-\log \mathcal{F}[\,g\,]\left(\tfrac{\cdot}{2\pi}\right))\right)^* \\
&= (-\log \mathcal{F}[\,f\,]\left(\tfrac{\cdot}{2\pi}\right))^* \,\square\, (-\log \mathcal{F}[\,g\,]\left(\tfrac{\cdot}{2\pi}\right))^* \\
&= \mathcal{C}_{\mathcal{F}}[\,f\,] \,\square\, \mathcal{C}_{\mathcal{F}}[\,g\,]
\end{aligned} \tag{53}$$

where we have applied the convolution theorem

$$\mathcal{F}[\,f * g\,] = \mathcal{F}[\,f\,]\,\mathcal{F}[\,g\,] \tag{54}$$

for the Fourier transform and the well known property

$$(f+g)^* = f^* \,\square\, g^* \tag{55}$$

of the convex conjugate. □ □

Taking a *delta peak* with $\boldsymbol{x}_0$ fixed

$$\delta(\boldsymbol{x}) = \begin{cases} 1 & \text{for } \boldsymbol{x} = 0 \\ 0 & \text{else} \end{cases} \tag{56}$$

as f, and the convolution kernel k of an LSI space-space as g, Theorem 1 shows that we obtain a morphological scale-space with structuring function $\mathcal{C}_{\mathcal{F}}[\,k\,]$ and *morphological delta peak*

$$\chi(\boldsymbol{x}) = \begin{cases} 0 & \text{for } \boldsymbol{x} = 0 \\ \infty & \text{else} \end{cases}. \tag{57}$$

as initial value. The morphological delta peak is the neutral element for infimal convolutions in the same way as a delta peak is the neutral element for convolutions.
For applications in image processing, we use the convolution kernels and these obtained structuring functions to create linear and morphological scale-spaces with the same initial image f.

Definition 2. *For some LSI scale-space*

$$u(\boldsymbol{x}, t) = (f * k(\cdot, t))(\boldsymbol{x}) \tag{58}$$

with convolution kernel

$$k(\boldsymbol{x},t) \;=\; \mathcal{F}^{-1}\left[\,\exp\left(p(2\pi\,\cdot)\,t\right)\right](\boldsymbol{x}) \tag{59}$$

and initial image f, the structuring function $s(\boldsymbol{x},t)$ for a corresponding morphological scale-space

$$v(\boldsymbol{x},t) = (f \,\square\, s(\cdot,t))(\boldsymbol{x}) \tag{60}$$

is obtained by applying the Cramér–Fourier transform to $k(\boldsymbol{x},t)$:

$$s(\boldsymbol{x},t) \;=\; \mathcal{C}_{\mathcal{F}}\left[\,k(\cdot,t)\,\right](\boldsymbol{x}) \;=\; \left(-t\,p(\cdot)\right)^{*}(\boldsymbol{x}). \tag{61}$$

4.2 Connections between Linear and Morphological Evolutions

Interestingly, we can also use the Cramér-Fourier transform on the level of evolution equations. This enables us to prove the following theorem which constitutes our main theoretical result.

Theorem 2 (Main Theorem)**.** *Let $u(\boldsymbol{x},t)$ be the solution of the LSI scale-space evolution*

$$\partial_t u(\boldsymbol{x},t) = p\left(\boldsymbol{\nabla}\right) u(\boldsymbol{x},t) \qquad \text{on } \mathbb{R}^2 \times (0,\infty) \tag{62}$$

$$u(\boldsymbol{x},0) = \delta(\boldsymbol{x}) \qquad \text{on } \mathbb{R}^2 \tag{63}$$

where $p(\boldsymbol{\xi})$ denotes the symbol of the pseudodifferential operator $P(\boldsymbol{\nabla})$ with constant coefficients.
If p is proper, lower semi-continuous and convex, the Cramér-Fourier transform of u, denoted by v, is the unique viscosity solution of the morphological scale-space evolution

$$\partial_t v(\boldsymbol{x},t) = p\left(\boldsymbol{\nabla} v(\boldsymbol{x},t)\right) \qquad \text{on } \mathbb{R}^2 \times (0,\infty) \tag{64}$$

$$v(\boldsymbol{x},0) = \chi(\boldsymbol{x}) \qquad \text{on } \mathbb{R}^2\,. \tag{65}$$

A similar theorem using the Cramér transform is proved by Akian et al. [2]. While their proof could be modified to our setting, using the previous obtained results is much simpler.

Proof. The discussion in Section 2.1 shows that the solution of (62)-(63) is given b which

$$u(\boldsymbol{x},t) = (\delta * k(\cdot,t))(\boldsymbol{x}) \tag{66}$$

with $k(\boldsymbol{x},t) = \mathcal{F}^{-1}[\exp(p(2\pi\cdot)t)](\boldsymbol{x})$. Since p is proper, lower semi-continuous and convex, applying Theorem 1 shows that $v(\boldsymbol{x},t) = \mathcal{C}_{\mathcal{F}}[u(\cdot,t)](\boldsymbol{x})$ is given by

$$v(\boldsymbol{x},t) = (\chi \,\Box\, s(\cdot,t))(\boldsymbol{x}) \tag{67}$$

with $s(\boldsymbol{x},t) = (-t\,p(\cdot)^*(\boldsymbol{x}))$. Following the discussion in Section 3.2 with $H = -p$, this is the Hopf-Lax formula for the unique viscosity solution of (64)-(65). □ □

This motivates us to introduce the following definition that is the counterpart of Definition 2 in terms of evolution equations.

Definition 3. *Let an LSI scale-space evolution be given by*

$$\partial_t u = P(\boldsymbol{\nabla})u\,, \tag{68}$$

$$u(\boldsymbol{x},0) = f(\boldsymbol{x})\,. \tag{69}$$

Then its corresponding morphological scale-space *evolution satisfies*

$$\partial_t v = p\left(\boldsymbol{\nabla} v\right)\,, \tag{70}$$

$$v(\boldsymbol{x},0) = f(\boldsymbol{x})\,. \tag{71}$$

Note that for computing the corresponding morphological scale-space, only the symbol p of the LSI scale-space is required. In particular, no closed form kernel representation is necessary.

Figure 1 summarises our main theoretical findings. We observe that we have obtained a simple dictionary that allows to translate results between linear and morphological scale-spaces, both in terms of convolutions / infimal convolutions and evolution equations.

5 Application to Specific Scale-Spaces

Now we are in a position to apply our theory to a number of linear scale-spaces in order to derive their morphological counterparts.

5.1 Gaussian Scale-Space

Table 1 specifies the symbol of Gaussian scale-space as

$$p(\boldsymbol{\xi}) = -|\boldsymbol{\xi}|^2\,. \tag{72}$$

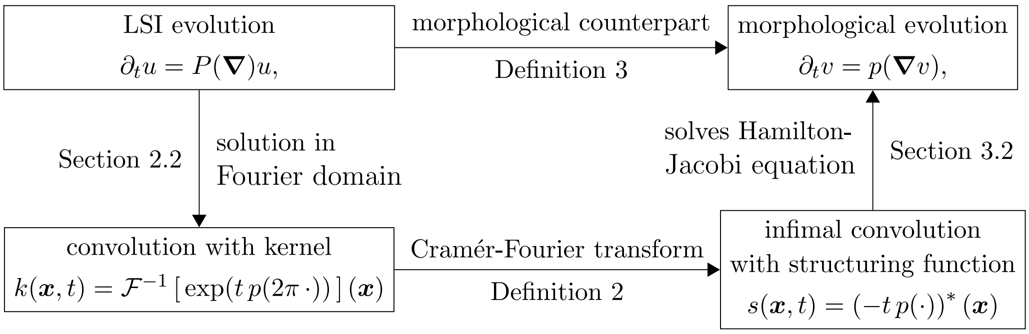

Figure 1: General dictionary that allows to translate results between LSI scale-spaces and morphological scale-spaces, both on the level of evolution equations (top) and the level of convolutions / infimal convolutions (bottom).

According to Definition 3, its morphological counterpart is given by

$$\partial_t v = -|\boldsymbol{\nabla} v|^2\,, \tag{73}$$

which coincides with van den Boomgaard's result [58]. According to our framework, the corresponding structuring function can be computed as

$$s(\boldsymbol{x}) = (-\,p\,(\cdot))^*\,(\boldsymbol{x}) = \tfrac{1}{4}|\boldsymbol{x}|^2, \tag{74}$$

which again confirms van den Boomgaard's result. This shows that our framework reproduces the only connection between linear and morphological scale-spaces that is known so far. Thus, we can focus now on establishing novel connections.

5.2 α-Scale-Spaces

In the same way as above, one can show that the morphological equivalents for the α-scale-spaces are given by

$$\partial_t v = -|\boldsymbol{\nabla} v|^{2\alpha}. \tag{75}$$

We observe that this is exactly the class of morphological evolutions that are studied by Jackway [29] and by Diop and Angulo [15].

Interestingly, (75) also proves that for $\alpha = \frac{1}{2}$, the linear counterpart of the widely-used morphological scale-space

$$\partial_t v = -|\boldsymbol{\nabla} v|, \tag{76}$$

which describe erosion with a flat disc of radius t, is given by the Poisson scale-space

$$\partial_t u = -\sqrt{-\Delta}\, u\,. \tag{77}$$

To our knowledge, this connection has not been stated before.

As a didactic example, let us now confirm that our computations also reproduce the structuring functions of [15]. Knowing the symbol $p(\boldsymbol{x}) = -|\boldsymbol{x}|^{2\alpha}$, we can use (28) again to compute s_α :

$$\begin{aligned} s_\alpha(\boldsymbol{x}) &= \left(-p\left(\cdot\right)\right)^*(\boldsymbol{x}) = (|\cdot|^{2\alpha})^*(\boldsymbol{x}) \\ &= (2\alpha-1)\left|\frac{\boldsymbol{x}}{2\alpha}\right|^{\frac{2\alpha}{2\alpha-1}}\,, \end{aligned} \tag{78}$$

since (see e.g. [51]), p. 106)

$$\left(\tfrac{1}{b}|\cdot|^b\right)^*(\boldsymbol{x}) = \tfrac{b-1}{b}|\boldsymbol{x}|^{\frac{b}{b-1}} \qquad \text{for } b > 1\,. \tag{79}$$

This coincides with the result from [15] stated in (44). Although this formula only holds for $\alpha > \frac{1}{2}$, we can compute the pointwise limit

$$\lim_{\alpha\to\frac{1}{2}^+} s_\alpha(\boldsymbol{x}) = \begin{cases} 0 & |\boldsymbol{x}| \leq 1, \\ \infty & \text{else.} \end{cases} \tag{80}$$

As expected, this is a flat disc of radius 1.

5.3 Summed α-Scale-Spaces

We know that summed α-scale-spaces have the symbol

$$p(\boldsymbol{\xi}) = -\sum_{k=1}^{m} \lambda_k |\boldsymbol{\xi}|^{2\alpha_k}\,. \tag{81}$$

This yields

$$\partial_t u = -\sum_{k=1}^{m} \lambda_k |\boldsymbol{\nabla} u|^{2\alpha_k} \tag{82}$$

as morphological counterpart of

$$\partial_t u = -\sum_{k=1}^{m} \lambda_k (-\Delta)^{\alpha_k}\, u\,. \tag{83}$$

In a similar way as before, its structuring function can be derived as

$$s(\boldsymbol{x}) = \mathop{\square}_{k=1}^{m} \lambda_k (2\alpha_k-1)\left|\frac{\boldsymbol{x}}{2\alpha_k\,\lambda_k}\right|^{\frac{2\alpha_k}{2\alpha_k-1}}\,. \tag{84}$$

5.4 Relativistic Scale-Spaces

From Table 1 we see that relativistic scale-spaces are characterised by the symbol

$$p(\boldsymbol{\xi}) = m - \sqrt{|\boldsymbol{\xi}|^2 + m^2}\,. \tag{85}$$

This gives

$$\partial_t v = m - \sqrt{|\boldsymbol{\nabla} v|^2 + m^2} \tag{86}$$

as morphological counterparts. The structuring function $s_{r,m}$ can be computed as before as the convex conjugate of the negative symbol:

$$s_{r,m}(\boldsymbol{x}) = \left(\sqrt{|\cdot|^2 + m^2} - m\right)^{*}(\boldsymbol{x}) \tag{87}$$

$$= \sup_{\boldsymbol{y}\in\mathbb{R}^2} \left(\langle \boldsymbol{x}, \boldsymbol{y}\rangle + m - \sqrt{|\boldsymbol{y}|^2 + m^2}\right). \tag{88}$$

If $|\boldsymbol{x}| \leq 1$, the solution for $\boldsymbol{y}$ is given by

$$\boldsymbol{y} = \frac{\boldsymbol{x}\, m}{1 - |\boldsymbol{x}|^2}\,. \tag{89}$$

Thus, it follows that

$$s_{r,m}(\boldsymbol{x}) = \begin{cases} m\left(1 - \sqrt{1 - |\boldsymbol{x}|^2}\right) & |\boldsymbol{x}| \leq 1, \\ \infty & \text{else.} \end{cases} \tag{90}$$

For $m \to 0$, the structuring function $s_{r,m}$ converges to a flat disc of radius 1. This is expected from the results from the last section, since the relativistic scale-spaces converge to the Poisson scale-space for $m \to 0$.

5.5 Anisotropic Scale-Spaces

The symbol for anisotropic Gaussian scale-space is

$$p(\boldsymbol{\xi}) = -\langle \boldsymbol{\xi}, \boldsymbol{D}\,\boldsymbol{\xi}\rangle\,. \tag{91}$$

This allows to compute the morphological counterpart of

$$\partial_t u = \operatorname{div}(\boldsymbol{D}\,\boldsymbol{\nabla} u) \tag{92}$$

as

$$\partial_t v = -\langle \boldsymbol{\nabla} v, \boldsymbol{D}\,\boldsymbol{\nabla} v\rangle\,. \tag{93}$$

As already mentioned, this morphological evolution has been studied by van den Boomgaard [57] and by Jackway [30].

So far we have always started with LSI scale-spaces and derived their corresponding morphological scale-space. The only morphological evolution that we could not derive in this way was the anisotropic differential equation of Arehart et al. [6]:

$$\partial_t v \;=\; -|\boldsymbol{D}\boldsymbol{\nabla} v| \;=\; -\sqrt{\boldsymbol{\nabla}^\top v\, \boldsymbol{D}^2\, \boldsymbol{\nabla} v}\,. \tag{94}$$

This is a good opportunity to show that our theoretical framework provides us with a dictionary that can be used also in the reverse direction. Obviously (94) can be expressed as

$$\partial_t v = p(\boldsymbol{\nabla} v) \tag{95}$$

with symbol

$$p(\boldsymbol{\xi}) = -\sqrt{\boldsymbol{\xi}^\top \boldsymbol{D}^2\, \boldsymbol{\xi}}\,. \tag{96}$$

This gives rise to an anisotropic Poisson scale-space

$$\partial_t u = -\sqrt{-\boldsymbol{\nabla}^\top \boldsymbol{D}^2\, \boldsymbol{\nabla}}\; u \tag{97}$$

that has not been described in the literature before.

Table 3 summarises the results of Section 5. We observe that we have derived many correspondences between known LSI scale-spaces and morphological ones. Moreover, we have also managed to come up with novel scale-spaces.

Table 3: Specific LSI scale-spaces and their morphological equivalents.

LSI scale-space	LSI evolution	morphological evolution	morphological scale-space
Gaussian	$\partial_t u = \Delta u$	$\partial_t v = -\lvert\boldsymbol{\nabla} v\rvert^2$	quadratic SF
Poisson	$\partial_t u = -\sqrt{-\Delta}\, u$	$\partial_t v = -\lvert\boldsymbol{\nabla} v\rvert$	flat disk SF
alpha	$\partial_t u = -(-\Delta)^\alpha u$	$\partial_t v = -\lvert\boldsymbol{\nabla} v\rvert^{2\alpha}$	poweroid SF
summed alpha	$\partial_t u = -\sum_{k=1}^m \lambda_k (-\Delta)^{\alpha_k} u$	$\partial_t v = -\sum_{k=1}^m \lambda_k \lvert\boldsymbol{\nabla} v\rvert^{2\alpha_k}$	morphological summed alpha
relativistic	$\partial_t u = \left(m - \sqrt{m^2 - \Delta}\,\right) u$	$\partial_t v = m - \sqrt{m^2 + \lvert\boldsymbol{\nabla} v\rvert^2}$	morphological relativistic
anisotropic Gaussian	$\partial_t u = \mathrm{div}(\boldsymbol{D}\,\boldsymbol{\nabla} u)$	$\partial_t v = -\boldsymbol{\nabla}^\top v\, \boldsymbol{D}\, \boldsymbol{\nabla} v$	anisotropic quadratic SF
anisotropic Poisson	$\partial_t u = -\sqrt{-\boldsymbol{\nabla}^\top \boldsymbol{D}^2\, \boldsymbol{\nabla}}\; u$	$\partial_t v = -\lvert\boldsymbol{D}\boldsymbol{\nabla} v\rvert$	flat ellipse-shaped SF

6 Experiments

Although our paper is of theoretical nature, we would like to illustrate some of the discussed scale-spaces and their correspondences by experiments.

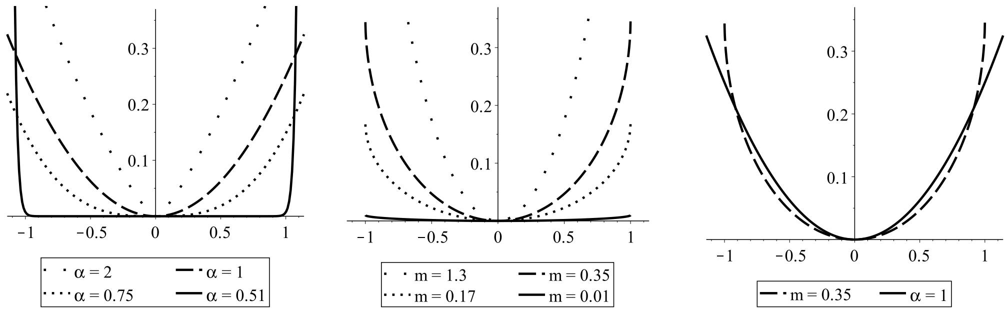

(a) morphological α-scale-space

(b) morphological relativistic scale-space

(c) morphological Gaussian and relativistic scale-space

Figure 2: Structuring functions for one-dimensional morphological scale-spaces.

The implementation for the linear scale-spaces uses a multiplication in the Fourier domain. For the morphological scale-spaces, we compute the infimal convolution over the image domain.

In Figure 2, we plot structuring functions of the morphological counterparts of various alpha- and relativistic scale-spaces. First of all, we observe the convexity of all structuring functions. Fig. 2(a) shows that for $\alpha \to 0.5$, the structuring function of the morphological α-scale-space converges to a flat structuring function. A similar behaviour can be observed for morphological relativistic scale-spaces when $m \to 0$; see Fig. 2(b). On the other hand, Fig. 2(c) shows that for $m = 0.4$, the morphological relativistic scale-space gives a good approximation to the morphological equivalent of Gaussian scale-space.

Figure 3 shows the two-dimensional linear α-scale-space for $\alpha = 0.75$ together with its morphological infimal convolution counterpart which corresponds to an erosion process. To enable comparisons, we have chosen the same Mona Lisa image as in [12]. Moreover, for the sake of completeness, we also depict the corresponding dilation scale-space.

Figure 4 compares the linear and morphological relativistic scale-space for $m = 0.1$. Since this m value is fairly close to the limit $m \to 0$, the linear evolution resembles Poisson scale-space, and its morphological counterpart approximates erosion with disc-shaped structuring functions. The latter is well visible.

The last example in Figure 5 shows that the anisotropy of the convolution kernel carries over to the structuring function. For this experiment we take

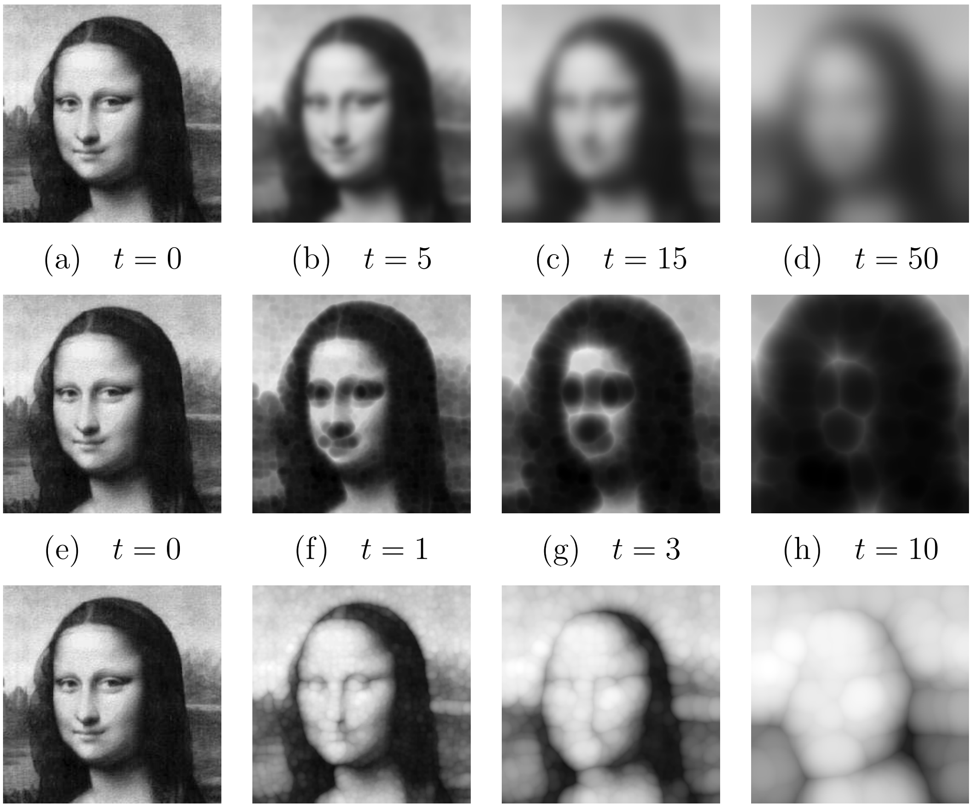

(a) $t = 0$ (b) $t = 5$ (c) $t = 15$ (d) $t = 50$

(e) $t = 0$ (f) $t = 1$ (g) $t = 3$ (h) $t = 10$

(i) $t = 0$ (j) $t = 1$ (k) $t = 3$ (l) $t = 10$

Figure 3: **Top:** Linear α-scale-space with $\alpha = 0.75$. **Middle:** Morphological α-scale-space with $\alpha = 0.75$. **Bottom:** Corresponding dilation scale-space.

the matrix

$$\boldsymbol{D} = \begin{pmatrix} 5 & 1 \\ 1 & 1 \end{pmatrix} \tag{98}$$

and compare the convolution kernel of the anisotropic Poisson scale-space to its corresponding flat, ellipse-shaped structuring function (45) with the inverse matrix

$$\boldsymbol{D}^{-1} = \frac{1}{4}\begin{pmatrix} 1 & -1 \\ -1 & 5 \end{pmatrix}. \tag{99}$$

7 Conclusions and Future Work

We have established a mathematical dictionary that allows to translate any linear shift-invariant scale-space evolution into its morphological counterpart

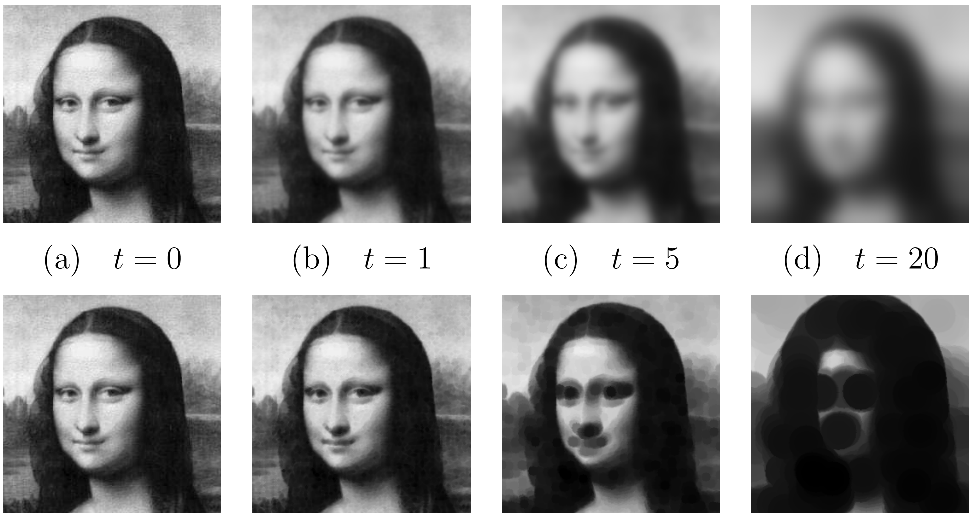

(a) $t = 0$ (b) $t = 1$ (c) $t = 5$ (d) $t = 20$

(e) $t = 0$ (f) $t = 1$ (g) $t = 5$ (h) $t = 20$

Figure 4: **Top:** Linear relativistic scale-space with $m = 0.1$. **Bottom:** Morphological relativistic scale-space with $m = 0.1$.

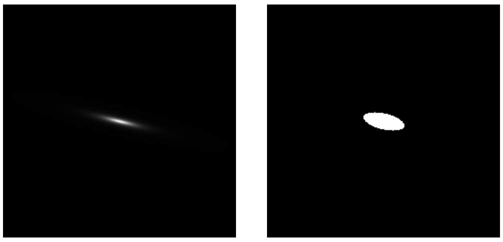

(a) $t = 3$ (b) $t = 10$

Figure 5: **Left:** Convolution kernel for linear anisotropic Poisson scale-space. **Right:** Corresponding structuring function.

of Hamilton-Jacobi type and vice versa. In contrast to previous work on structural similarities between linear and morphological systems, we have achieved these equivalences in the terminology of differential or pseudodifferential operators. It turned out that the symbol p is a very simple and powerful concept: It allows to transform the linear evolution equation $\partial_t u = P(\boldsymbol{\nabla})u$ into its morphological counterpart $\partial_t v = p(\boldsymbol{\nabla} v)$. By considering specific examples of linear or morphological scale-spaces we have discovered hitherto unexplored relations between known scale-spaces, such as the Poisson scale-space and morphology with a disc-shaped structuring element of increasing size. Moreover, novel scale-spaces have been introduced that have not been studied before, e.g. anisotropic Poisson scale-spaces and morphological relativistic scale-spaces.

There are numerous ways to extend our findings in interesting directions. Obviously, these new scale-spaces should be explored further in order to identify promising applications. On the other hand, it is also challenging to extend the current applications and limitations of our dictionary, e.g. by considering to Lie group versions of linear scale-spaces [17, 18]. So far, our framework requires evolutions that adhere to a semi-group property. This excludes its application to scale-spaces that do not satisfy this requirement, e.g. regularisation scale-spaces [13, 44, 50, 53] and the closely related Bessel scale-space [10]. We will investigate if our concepts can be extended to handle also these processes. Another current limitation is the restriction to linearity on the classical scale-space side due to the involvement of the Fourier transform. If we can overcome this limitation, also nonlinear scale-spaces such as nonlinear diffusion [49, 60] and curvature-based morphological evolutions [3, 4, 33, 52] can be studied. These are topics of our ongoing research.

Acknowledgements Our research on this topic has been initiated by discussions between Joachim Weickert and Bernd Sturmfels (Berkeley) during the DEMAIN Conference in Münster (Sept. 30 – Oct. 2, 2014). It is a pleasure to thank Angela Stevens (Münster) for organising this highly inspiring interdisciplinary conference.

References

[1] Abramowitz, M., Stegun, I.A.: Handbook of Mathematical Functions with Formulas, Graphs, and Mathematical Tables. Dover, New York (1974)

[2] Akian, M., Quadrat, J., Viot, M.: Bellman processes. In: ICAOS '94: Discrete Event Systems, *Lecture Notes in Control and Information Sciences*, vol. 199, pp. 302–311. Springer, London (1994)

[3] Alvarez, L., Guichard, F., Lions, P.L., Morel, J.M.: Axioms and fundamental equations in image processing. Archive for Rational Mechanics and Analysis **123**, 199–257 (1993)

[4] Alvarez, L., Lions, P.L., Morel, J.M.: Image selective smoothing and edge detection by nonlinear diffusion. II. SIAM Journal on Numerical Analysis **29**, 845–866 (1992)

[5] Angulo, J.: Pseudo-morphological image diffusion using the counter-harmonic paradigm. In: J. Blanc-Talon, D. Bone, W. Philips, D. Popescu, P. Scheunders (eds.) Advanced Concepts for Intelligent Vision Systems, *Lecture Notes in Computer Science*, vol. 6474, pp. 426–437. Springer, Berlin (2010)

[6] Arehart, A.B., Vincent, L., Kimia, B.B.: Mathematical morphology: The Hamilton–Jacobi connection. In: Proc. Fourth International Conference on Computer Vision, pp. 215–219. IEEE Computer Society Press, Berlin (1993)

[7] Baccelli, F., Cohen, G., Olsder, G.J., Quadrat, J.: Synchronization and Linearity: An Algebra for Discrete Event Systems. Wiley, Chichester (1992)

[8] Breuß, M., Burgeth, B., Weickert, J.: Anisotropic continuous-scale morphology. In: J. Martí, J.M. Benedí, A. Mendonça, J. Serrat (eds.) Pattern Recognition and Image Analysis, *Lecture Notes in Computer Science*, vol. 4478, pp. 515–522. Springer, Berlin (2007)

[9] Brockett, R.W., Maragos, P.: Evolution equations for continuous-scale morphology. In: Proc. IEEE International Conference on Acoustics, Speech and Signal Processing, vol. 3, pp. 125–128. San Francisco, CA (1992)

[10] Burgeth, B., Didas, S., Weickert, J.: The Bessel scale-space. In: O. Olsen, L. Florack, A. Kuijper (eds.) Deep Structure, Singularities, and Computer Vision, *Lecture Notes in Computer Science*, vol. 3753, pp. 84–95. Springer, Berlin (2005)

[11] Burgeth, B., Didas, S., Weickert, J.: Relativistic scale-spaces. In: R. Kimmel, N. Sochen, J. Weickert (eds.) Scale Space and PDE Methods in Computer Vision, *Lecture Notes in Computer Science*, vol. 3459, pp. 1–12. Springer, Berlin (2005)

[12] Burgeth, B., Weickert, J.: An explanation for the logarithmic connection between linear and morphological system theory. International Journal of Computer Vision **64**(2/3), 157–169 (2005)

[13] Demetz, O., Weickert, J., Bruhn, A., Zimmer, H.: Optic flow scale-space. In: A.M. Bruckstein, B. ter Haar Romeny, A.M. Bronstein, M.M. Bronstein (eds.) Scale Space and Variational Methods in Computer Vision, *Lecture Notes in Computer Science*, vol. 6667, pp. 713–724. Springer, Berlin (2012)

[14] Didas, S., Burgeth, B., Imiya, A., Weickert, J.: Regularity and scale-space properties of fractional high order linear filtering. In: R. Kimmel, N. Sochen, J. Weickert (eds.) Scale Space and PDE Methods in Computer Vision, *Lecture Notes in Computer Science*, vol. 3459, pp. 13–25. Springer, Berlin (2005)

[15] Diop, E.H., Angulo, J.: Multiscale image analysis based on robust and adaptive morphological scale-spaces. Image Analysis & Stereology **34**(1), 39–50 (2014)

[16] Dorst, L., van den Boomgaard, R.: Morphological signal processing and the slope transform. Signal Processing **38**, 79–98 (1994)

[17] Duits, R., Burgeth, B.: Scale spaces on Lie groups. In: F. Sgallari, A. Murli, N. Paragios (eds.) Scale Space and Variational Methods in Computer Vision, *Lecture Notes in Computer Science*, vol. 4485, pp. 300–312. Springer, Berlin (2007)

[18] Duits, R., DelaHaije, T., Creusen, E., Ghosh, A.: Morphological and linear scale spaces for fiber enhancement in DW-MRI. Journal of Mathematical Imaging and Vision **46**(3), 326–368 (2013)

[19] Duits, R., Florack, L., de Graaf, J., ter Haar Romeny, B.: On the axioms of scale space theory. Journal of Mathematical Imaging and Vision **20**, 267–298 (2004)

[20] Felsberg, M., Sommer, G.: Scale-adaptive filtering derived from the Laplace equation. In: B. Radig, S. Florczyk (eds.) Pattern Recognition, *Lecture Notes in Computer Science*, vol. 2032, pp. 95–106. Springer, Berlin (2001)

[21] Florack, L.: Image Structure, *Computational Imaging and Vision*, vol. 10. Kluwer, Dordrecht (1997)

[22] Florack, L.M.J., Maas, R., Niessen, W.J.: Pseudo-linear scale-space theory. International Journal of Computer Vision **31**(2/3), 247–259 (1999)

[23] Guichard, F., Morel, J.M.: Partial differential equations and image iterative filtering. In: I.S. Duff, G.A. Watson (eds.) The State of the Art in Numerical Analysis, no. 63 in IMA Conference Series (New Series), pp. 525–562. Clarendon Press, Oxford (1997)

[24] Heijmans, H.J.A.M.: Morphological scale-spaces, scale-invariance and Lie groups. In: H. Talbot, R. Beare (eds.) International Symposium on Mathematical Morphology, pp. 253–264 (2002)

[25] Heijmans, H.J.A.M., Maragos, P.: Lattice calculus of the morphological slope transform. Signal Processing **59**(1), 17 – 42 (1997)

[26] Iijima, T.: Basic theory on normalization of pattern (in case of typical one-dimensional pattern). Bulletin of the Electrotechnical Laboratory **26**, 368–388 (1962). In Japanese

[27] Iijima, T.: Basic theory on normalization of two-dimensional visual pattern. Studies on Information and Control (IECE, Japan) (1), 15–22 (1963). Pattern Recognition Issue. In Japanese

[28] Iijima, T.: Basic equation of figure and observational transformation. Systems, Computers, Controls **2**(4), 70–77 (1971). In English

[29] Jackway, P.T.: Properties of multiscale morphological smoothing by poweroids. Pattern Recognition Letters **15**(2), 135 – 140 (1994)

[30] Jackway, P.T.: On dimensionality in multiscale morphological scale-space with elliptic poweroid structuring functions. Journal of Visual Communication and Image Representation **6**(2), 189 – 195 (1995)

[31] Jackway, P.T., Deriche, M.: Scale-space properties of the multiscale morphological dilation–erosion. IEEE Transactions on Pattern Analysis and Machine Intelligence **18**, 38–51 (1996)

[32] Kanters, F., Florack, L., Duits, R., Platel, B., Haar Romeny, B.: ScaleSpaceViz: α-scale spaces in practice. Pattern Recognition and Image Analysis **17**(1), 106–116 (2007)

[33] Kimia, B.B., Siddiqi, K.: Geometric heat equation and non-linear diffusion of shapes and images. Computer Vision and Image Understanding **64**, 305–322 (1996)

[34] Koenderink, J.J.: The structure of images. Biological Cybernetics **50**, 363–370 (1984)

[35] Landström, A.: An approach to adaptive quadratic structuring functions based on the local structure tensor. In: J.A. Benediktsson, J. Chanussot, L. Najman, H. Talbot (eds.) Mathematical Morphology and Its Applications to Signal and Image Processing, *Lecture Notes in Computer Science*, vol. 9082, pp. 729–740. Springer (2015)

[36] Lindeberg, T.: Scale-Space Theory in Computer Vision. Kluwer, Boston (1994)

[37] Lindeberg, T.: Generalized Gaussian scale-space axiomatics comprising linear scale-space, affine scale-space and spatio-temporal scale-space. Journal of Mathematical Imaging and Vision **40**, 36–81 (2011)

[38] Lions, P.L.: Generalized Solutions of Hamilton-Jacobi Equations, *Research Notes In Mathematics*, vol. 69. Pitman, London (1992)

[39] Lowe, D.L.: Distinctive image features from scale-invariant keypoints. International Journal of Computer Vision **60**(2), 91–110 (2004)

[40] Lyons, R.G.: Understanding Digital Signal Processing. Prentice Hall, Englewood Cliffs (2004)

[41] Maclagan, D., Sturmfels, B.: Introduction to Tropical Geometry, *Graduate Studies in Mathematics*, vol. 161. AMS, Providence (2015)

[42] Maragos, P.: Morphological systems: Slope transforms and max-min difference and differential equations. Signal Processing **38**(1), 57–77 (1994)

[43] Maragos, P., Schafer, R.: Morphological filters–Part I: Their set-theoretic analysis and relations to linear shift-invariant filters. IEEE Transactions on Acoustics, Speech, and Signal Processing **35**(8), 1153–1169 (1987)

[44] Nielsen, M., Florack, L., Deriche, R.: Regularization, scale-space and edge detection filters. Journal of Mathematical Imaging and Vision **7**, 291–307 (1997)

[45] Olsen, O., Florack, L., Kuijper, A. (eds.): Deep Structure, Singularities, and Computer Vision, *Lecture Notes in Computer Science*, vol. 3753. Springer, Berlin (2005)

[46] Oppenheim, A.V., Schafer, R.W., Buck, J.R.: Discrete-Time Signal Processing, second edn. Prentice Hall, Englewood Cliffs (1999)

[47] Otsu, N.: Mathematical studies on feature extraction in pattern recognition. Tech. Rep. 818 (PhD Thesis), Electrotechnical Laboratory, Tsukuba, Japan (1981). In Japanese.

[48] Pauwels, E.J., Van Gool, L.J., Fiddelaers, P., Moons, T.: An extended class of scale-invariant and recursive scale space filters. IEEE Transactions on Pattern Analysis and Machine Intelligence **17**, 691–701 (1995)

[49] Perona, P., Malik, J.: Scale space and edge detection using anisotropic diffusion. IEEE Transactions on Pattern Analysis and Machine Intelligence **12**, 629–639 (1990)

[50] Poggio, T., Voorhees, H., Yuille, A.: A regularized solution to edge detection. Journal of Complexity **4**(2), 106 – 123 (1988)

[51] Rockafellar, R.T.: Convex Analysis. Princeton University Press, Princeton (1970)

[52] Sapiro, G., Tannenbaum, A.: Affine invariant scale-space. International Journal of Computer Vision **11**, 25–44 (1993)

[53] Scherzer, O., Weickert, J.: Relations between regularization and diffusion filtering. Journal of Mathematical Imaging and Vision **12**(1), 43–63 (2000)

[54] Schmidt, M., Weickert, J.: The morphological equivalents of relativistic and alpha-scale-spaces. In: J. Aujol, M. Nikolova, N. Papadakis (eds.) Scale Space and Variational Methods in Computer Vision, *Lecture Notes in Computer Science*, vol. 9087, pp. 28–39. Springer, Berlin (2015)

[55] Sporring, J., Nielsen, M., Florack, L., Johansen, P. (eds.): Gaussian Scale-Space Theory, *Computational Imaging and Vision*, vol. 8. Kluwer, Dordrecht (1997)

[56] Taylor, M.: Partial Differential Equations II: Qualitative Studies of Linear Equations. Applied Mathematical Sciences. Springer, New York (2010)

[57] van den Boomgaard, R.: Mathematical morphology: Extensions towards computer vision. Ph.D. thesis, University of Amsterdam, The Netherlands (1992)

[58] van den Boomgaard, R.: The morphological equivalent of the Gauss convolution. Nieuw Archief Voor Wiskunde **10**(3), 219–236 (1992)

[59] van den Boomgaard, R., Smeulders, A.: The morphological structure of images: The differential equations of morphological scale-space. IEEE

Transactions on Pattern Analysis and Machine Intelligence **16**, 1101–1113 (1994)

[60] Weickert, J.: Anisotropic Diffusion in Image Processing. Teubner, Stuttgart (1998)

[61] Weickert, J., Ishikawa, S., Imiya, A.: Linear scale-space has first been proposed in Japan. Journal of Mathematical Imaging and Vision **10**(3), 237–252 (1999)

[62] Welk, M.: Families of generalised morphological scale spaces. In: L. Griffin, M. Lillholm (eds.) Scale Space Methods in Computer Vision, *Lecture Notes in Computer Science*, vol. 2695, pp. 770–784. Springer, Berlin (2003)

[63] Witkin, A.P.: Scale-space filtering. In: Proc. Eighth International Joint Conference on Artificial Intelligence, vol. 2, pp. 945–951. Karlsruhe, West Germany (1983)